Author(s): Suhonen, Aku; Kortelainen, Minna; Nauha, Elisa; Yliniemelä-Sipari, Sanna; Pihko, Petri; Nissinen, Maija

Title: Conformational properties and folding analysis of a series of seven oligoamide foldamers

Year: 2016

Version:

Please cite the original version:

Suhonen, A., Kortelainen, M., Nauha, E., Yliniemelä-Sipari, S., Pihko, P., & Nissinen, M. (2016). Conformational properties and folding analysis of a series of seven oligoamide foldamers. CrystEngComm, 18(11), 2005-2013. https://doi.org/10.1039/C5CE02458G

Journal Name

ARTICLE

Conformational Properties and Folding Analysis of a Series of Seven Oligoamide Foldamers

Received 00th January 20xx,
Accepted 00th January 20xx

DOI: 10.1039/x0xx00000x

www.rsc.org/

Aku Suhonen, Minna Kortelainen, Elisa Nauha, Sanna Yliniemelä-Sipari, Petri M. Pihko and Maija Nissinen*

33 crystal structures (11 unsolvated and 22 solvates) of a series of seven oligoamide foldamers were analysed. The crystal structures revealed that despite the structural and environmental differences the series of foldamers prefer only two general conformations, a protohelical @-conformation and a sigmoidal S-conformation. Both conformations have also preferred crystal packing motifs and solvate forming tendencies. Hydrogen bonding was found to be the most decisive factor in conformational preference, but steric properties, the type of the peripheral substituents, as well as solvent and aromatic interactions were also found to have an effect on the conformational details and crystal form.

Introduction

Foldamers are biomimetic molecular scaffolds composed of relatively simple repeating structural units, which makes their secondary structure somewhat predictable.[1,2] Foldamers are generally considered as artificial models for molecular folding,[3] but they may also find use in enzyme-like functions, for example as biomimetic receptors[4] and catalysts[5,6,7]. The most common bond type in foldamers is the amide bond with directional and relatively stable hydrogen bonding properties. Hydrogen bonding, and therefore also the molecular folding and crystal packing networks, are affected by the electronic environment created by the nearby functional groups with contribution from other possible weak interactions, hydrophobic forces and close packing effects.

Aromatic oligoamides present a promising class of foldamers because of their structural rigidity, functionalization potential, and the predictability of the hydrogen bonding properties of the amide bonds. Many studies have been conducted on the preparation, solution state folding and functionalization of a variety of aromatic amide foldamers; for example, helical pyridine-2,6-dicarboxamide and *N,N*-pyridine-2,6-formamide foldamers by Lehn *et al.*[8,9] and Huc *et al.*,[10,11] 1-3 stranded helices of quinoline and naphthyridine foldamers by Huc *et al.*,[12,13,14,15,16] and aromatic oligoanthranilamides by Hamilton *et al.*[17,18] Single crystal X-ray diffraction studies have provided an important model and often a starting point for the determination of the solution state conformations of the foldamers. An in-depth understanding about the intermolecular interactions in the solid state and packing effects affecting the folding and conformational properties is therefore important to help to differentiate the conformational properties originating from the high density of the crystal structures from the universal conformational features and properties of the foldamer.

In our previous studies, we investigated the conformational variance of a series of oligoamide foldamers by computational, single crystal X-ray diffraction and NMR spectroscopic methods.[19,20] The oligoamide foldamers were able to adopt a conformation – among other almost equally stable conformers – where three intramolecular hydrogen bonds are formed to single carbonyl oxygen, closely resembling an oxyanion hole motif found in the active sites of enzymes[21]. In enzymes, an oxyanion hole motif consists of two or more hydrogen bond donors, which can form hydrogen bonds to a negatively charged oxygen atom of a reaction intermediate thus stabilising it and lowering the energy cost of the reaction. The examples of non-peptidic systems mimicking this behaviour are still scarce, only a few examples of amide and ester carbonyls acting as an acceptor for multiple hydrogen bonds have been reported.[22,23]

Our previous studies showed that relatively small alterations in chemical structure and crystallization conditions have an effect on the preferred folding patterns of oligoamides, but the calculated energy difference between the observed folding patterns is very small.[20] Herein we present a more detailed solid state structural study of a series of seven oligoamide foldamers (Scheme 1) summarizing their conformational features, polymorphism and solvate formation, as well as the variance in crystal packing caused by the conformational preferences, small changes in their chemical structure and crystallization conditions.

Nanoscience Center, Department of Chemistry, University of Jyvaskyla, P.O. BOX 35 40014 JYU, Finland. E-mail: maija.nissinen@jyu.fi; Tel: +358 50 428 0804

Electronic Supplementary Information (ESI) available: Synthesis and NMR spectra of foldamer **3**, selected PXRD patterns, notes on the crystallization and crystallographic data including isomorphous crystal structures, hydrogen bonding parameters of the structures and additional figures, TGA-DTA graph of compound **2**-Form III. CIF files of the crystal structures. CCDC reference numbers 1436659-1436674 and 1438546. See DOI: 10.1039/x0xx00000x.

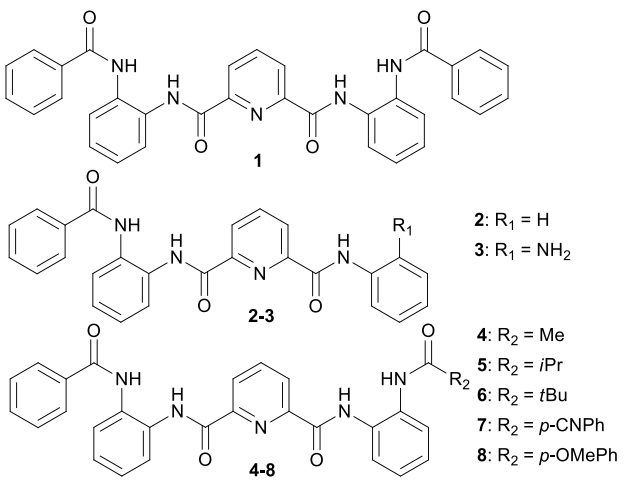

Scheme 1 Symmetrical oligoamide **1** and a series of asymmetric oligoamides **2**-**8**.

Results and Discussion

Folding patterns

The protohelical @-conformation originally found with compound **1**[19] provided an inspiration for the synthesis and folding studies of seven asymmetric analogues **2**-**8**[20] (Scheme 1) with different hydrogen bonding properties and electron donating and withdrawing end groups. Foldamers **2** and **3** are shorter and lack one amide group at one end of the molecule. Foldamer **3**, however, has an amine group capable of hydrogen bonding at the ortho-position of the short end. The methyl (**4**), isopropyl (**5**) and *tert*-butyl (**6**) groups increase the electron density at the adjacent C=O group and show increasing steric hindrance, which affects their molecular conformation. Foldamers **7** and **8** have five aromatic rings connected by four amide bonds like foldamer **1** but also an electron density withdrawing cyano group (**7**) or, electron density donating methoxy group (**8**) attached to the para position at one end of the molecule.

Foldamers **1-7** fold into two distinct conformations, denoted as @- and S-conformations according to our previous article[20] (Scheme 2). Foldamers **2**, **5** and **7** were found to adopt both conformations, whereas foldamers **1** and **3** crystallized exclusively in the @-conformation and foldamers **4** and **6** only in the S-conformation. No crystal structures could be obtained for foldamer **8** despite several attempts in various solvents. In the @-conformation, the oligoamide folds tightly around the pyridine core and forms two or three intramolecular hydrogen bonds to the same carbonyl oxygen (S(7), S(13) and S(16) motifs). In the conformational notation the number of hydrogen bonds is specified by an apostrophe, which designates that only two intramolecular hydrogen bonds are formed.

In the S-conformation, the molecule has a sigmoidal shape. One intramolecular hydrogen bond is formed from an outer amide N-H to an inner amide C=O (S(7) motif) and two intramolecular hydrogen bonds are formed between the N-H groups next to pyridine, and the other outer amide C=O (S(7) and S(13) motifs). Additionally, in all structures two weak intramolecular hydrogen bonds from the central pyridine ring nitrogen to the inner amide bond N-H groups form (S(5) motif). Both S- and @-conformers are further divided in categories 1 or 2 depending on which end of the molecule acts as a hydrogen bond acceptor to the pyridine core amide hydrogen bonds (Scheme 2).

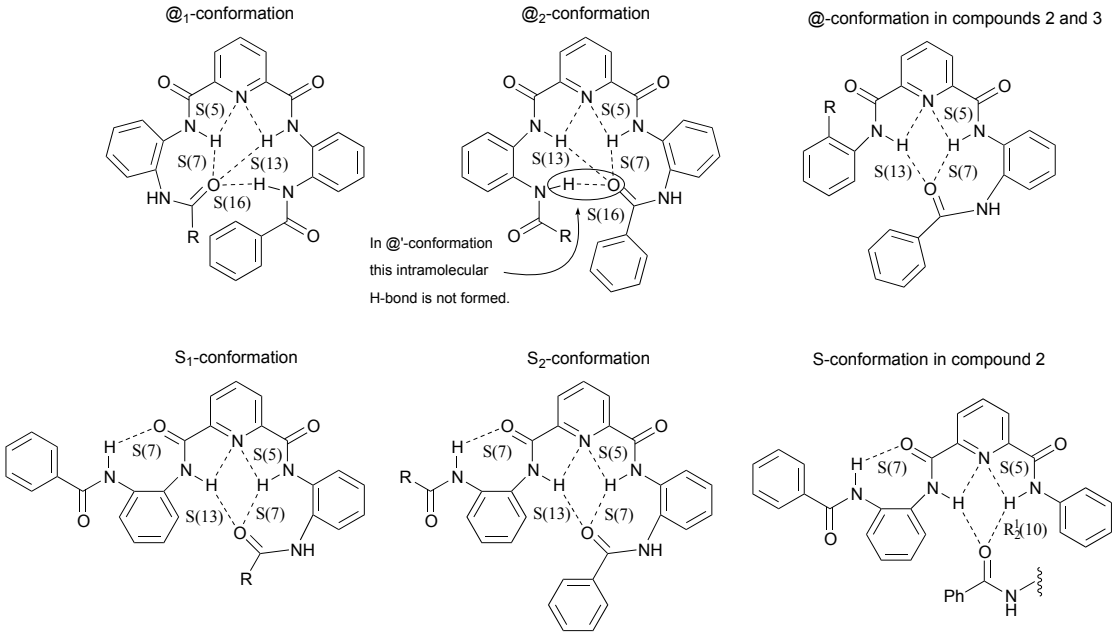

Scheme 2 Schematic representation of denotations of @ and S conformations. Subscripts describe which of the available carbonyls groups act as a hydrogen bond donor. With the smallest foldamers **2** and **3** only one type of @ conformation is possible and S conformer may also form via intermolecular hydrogen bonding.

Table 1. Crystal packing, packing coefficients and crystallizations solvents of the crystal structures of **1**-**7**.

Structure:	Packing motif:	Packing coefficient:	Coefficient Δ:	Crystallization solvent:
1@-Form I[19]	$R_2^2(14)$	0.7116	0.034330	EtOAc
1@-Form II	$R_4^4(46), 2R_3^3(39)$	0.7270	0.018985	DMSO-d_6, 1:TBA-F 3H_2O (5:1)
1@-Ac	C(7)	0.7312	0.014780	Acetone-d_6, 1:TBA-Cl (3:1)
1@-DMA	C(7)	0.7374	0.008502	DMA
1@-DMF[19]	C(7)	0.7351	0.010803	DMF
1@-DMSO[19]	C(11)	0.7091	0.036808	DMSO
1@-DMSO-H_2O	C(7),$D_2^2(5)$	0.7459	0	DMSO-d_6, 1:TBA-F 3H_2O (1:4)
1@-EtOAc[19]	C(11)	0.6988	0.047159	EtOAc
1@-EtOH[19]	C(16)	0.7306	0.015293	EtOH
1@-MeCN	C(7)	0.7238	0.022152	MeCN
1@-MeOH[19]	C(16)	0.7317	0.014228	MeOH
1@-toluene[19]	C(11)	0.7011	0.044861	Toluene
2@-Form I[20]	C(11)	0.7121	0.018715	Acetone
2@-Form II	C(7)	0.7308	0	DMA
2S-DCM-1	$2R_2^1(10)$	0.6982	0.032628	DCM
2S-DCM-2	$2R_2^1(10)$	0.6984	0.032443	DCM
2@-DMA	D	0.7220	0.008799	DMA
2@-**S**-DMF[20]	$R_2^2(14), 2R_2^1(10)$	0.7200	0.010860	DMF
2S-MeCN[20]	$2R_2^1(10)$	0.7145	0.016341	MeCN
3@-Form I	$C_2^1(16)$	0.7224	0	Acetone
4S$_1$-Form I[20]	$R_2^2(32)$	0.7106	0.028646	Acetone
4S$_1$-Form II	$R_2^2(32)$	0.7146	0.024712	EtOAc
4S$_1$-Diox	$R_2^2(32)$	0.7393	0	1,4-Dioxane
4S$_1$-DMSO	D	0.7189	0.020415	DMSO
5@'$_2$-Form I[20]	$C_2^2(23)$	0.7254	0	EtOAc
5S$_1$-Form II[20]	$R_2^2(14)$	0.699	0.025490	Toluene
6S$_2$-Form I[20]	C(11)	0.7151	0.008387	Acetone
6S$_2$-Diox	C(11))	0.7235	0	1,4-Dioxane
7@$_2$-Form I[20]	C(7)	0.7253	0	MeCN
7S$_1$-$CHCl_3$	$R_2^2(14)$	0.6811	0.044256	$CHCl_3$
7S$_1$-DMA	$R_2^2(14)$	0.7096	0.015744	DMA
7S$_1$-EtOAc[20]	$R_2^2(14)$	0.7135	0.011822	EtOAc
7S$_1$-THF	$R_2^2(14)$	0.6911	0.034294	THF

The main reason behind the popularity of the proto-helical @-conformation and the sigmoidal S-conformation are the several simultaneous intramolecular hydrogen bonds, which stabilize the conformers almost equally, as evidenced by DFT calculations[20] and the prevalence of both conformers in the crystal structures. The steric effects are likely to contribute to the conformation as well, especially in the case of foldamer **6** with a bulkier aliphatic group, which lead to a slight preference of more open and less compact S-conformer to minimize the steric strain.

The effect of intramolecular aromatic interactions on the conformational properties is surprisingly small: although DFT calculations indicated stabilising aryl-aryl interactions, none are seen in the S-conformer structures, and only one or two weak T-stacking interactions are present and contribute to the stabilities of the @-conformers.

Structural analysis of individual compounds

Foldamer 1

Foldamer **1** proved to be a very versatile source of good quality crystals. Altogether 12 different crystal structures have been obtained for foldamer **1**: two polymorphs (previously published **1**@-Form I[19] and **1**@-Form II) and ten solvates with varying types of solvents, six of which are published previously[19]. The versatility of crystal formation was observed as nearly identical crystallization conditions produced several different crystal forms. The crystallization experiments from DMSO solutions, for example, have produced three different crystal forms: unsolvated form II, DMSO/H_2O solvate and a DMSO solvate[19]. Ethyl acetate and acetonitrile crystallizations produced both **1**@-Form I, and respective solvates. However, some tendency to favour certain crystal forms according to solvent size and type was observed: DMF, DMA, acetonitrile and acetone solvates are isomorphous, as are also ethanol and methanol solvates and ethyl acetate and toluene solvates. A common theme in all crystal structures is still the tendency to strongly favour the @-conformation (Table 1, Figure 1a) with

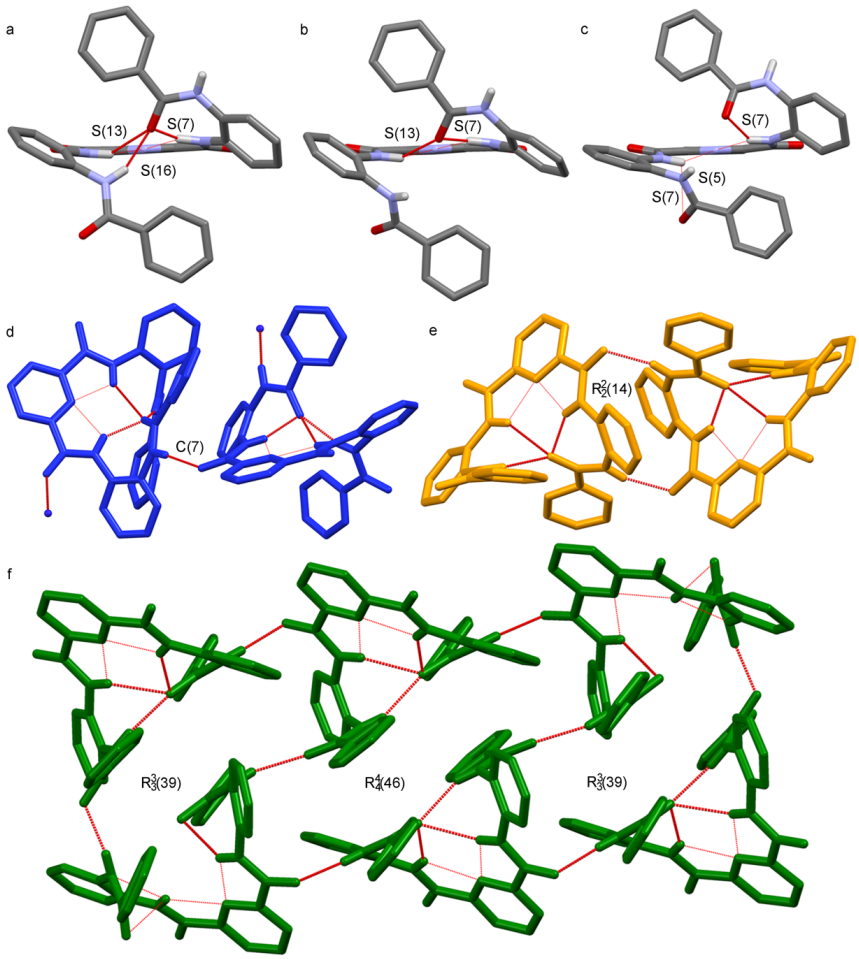

Fig. 1. Variance in @-conformation of foldamer **1** a) @-conformation (**1@**-DMSO-H_2O), b) @'-conformation (**1@'**-DMSO)[20] and c) open @-like conformation (**1@**-Form II). Examples of foldamer **1** crystal packing d) a chain packing structure (C(7) motif, **1@**-DMA), e) a pair ring structure ($R_2^2(14)$motif **1@**-Form I) and f) six molecule double ring structure ($R_4^4(46)2R_3^3(39)$ motif, **1@**-Form II).

only a slight variation of conformational details: all other structures produce identical @-fold except for **1**@-Form II and **1**@-DMSO. In **1**@-Form II the asymmetric unit contains three molecules, one of which is not in a perfect @-conformation, but instead in a more open conformation, which nevertheless closely resembles the @-conformation (Figure 1c). This conformer has fewer and weaker hydrogen bonds and a different intramolecular hydrogen bond network (two S(7) motifs and S(5) motif). The @-conformer of foldamer **1** in the DMSO solvate[19] is classified as an @'-conformation (Figure 1b) as a slight twisting of the amide bond at the other end of the molecule prohibits the formation of a third hydrogen bond. Instead, the hydrogen bond is formed to a DMSO solvent molecule.

The crystal packing of the solvate structures of foldamer **1** favour chain-like motifs typical for most @-conformation structures, whereas two polymorphic forms, **1**@-Form I and **1**@-Form II, adopt a ring like packing motif. In **1**@-Form I the packing is based on pairs ($R_2^2(14)$ motif) and in **1**@-Form II as a triple ring formed by six molecules ($2R_3^3(39), R_4^4(46)$ motifs; Table 1, Figure 1e and ESI).

Foldamer 2

The lack of the fourth amide bond in foldamer **2** does not hinder the folding of the molecule and foldamer **2** crystallizes equally in @- and S-conformations (Figure 2). A fast overnight crystallization from DMF even produced a structure with both conformers present in the same crystal (Table 1), which indicates that the conformers are indeed close in energy as suggested by DFT calculations.[20]

In five different solvates obtained both conformers are observed and no clear solvent dependent pattern of which conformer crystallizes out is seen. As with foldamer **1** the same solvent could produce several different crystal structures (see ESI for details), which also indicates that during the crystal nucleation the molecule is able to adopt both conformers depending on the conditions and the most favourable interactions. Notably, foldamer **2** adopts the S-conformer through intermolecular hydrogen bonding to an adjacent molecule instead of the intramolecular hydrogen bonding, thus forming a dimeric pair typical for S-conformers (Scheme 3, Figure 2c). The crystal packing of @-conformer structures

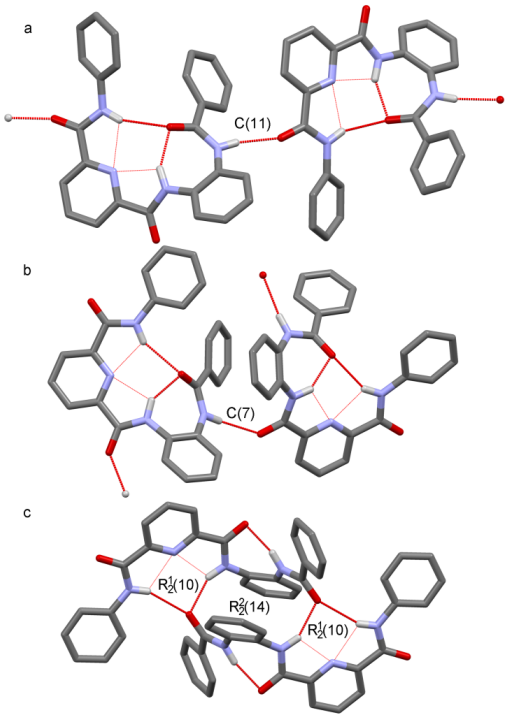

Fig. 2. Crystal packing of foldamer **2**. a) Chain structure of **2**@-Form I (C(11) motif), b) Chain structure of **2**@-Form II (C(7) motif) and c) S-conformation pair structure ($2R_2^1(10)$ motif, **2**S-DCM-1).

follows the general trends, as @-conformers pack into chains (Figure 2a and 2b).

Foldamer 3

Despite the close structural and chemical resemblance of foldamer **3** to foldamer **2** its crystallization modes were very different. Although several solvents and solvent mixtures were used (see ESI for details), and numerous crystallization attempts were made, foldamer **3** repeatedly crystallized as the same unsolvated @-conformation structure, if the suitable quality crystals were obtained (Figure 3). The conformation resembles closely the @-conformation of foldamer **2** and the additional amine group does not participate in intramolecular bonding. Instead, the amine group is involved in forming a double chain crystal packing motif, which is likely very stable due to multiple hydrogen bonds and also the reason why only one crystal form is observed.

Foldamer 4

Foldamer **4** was exclusively found in the S_1-conformation both as polymorphs (**4**S_1-Form I and **4**S_1-Form II) and as two solvates (with DMSO and dioxane; Table 1). The result is surprising as the CH_3 group is small and provides only little steric hindrance for folding into an @-conformation. The prevalence of type 1 interactions (Scheme 3) can be rationalized by the fact that the methyl group at the acetyl moiety slightly increases the electron density of the closest C=O group thus making it more favourable as a hydrogen bond acceptor. The crystal form **4**S_1-Form I appears to be the most stabile of the structures, as,

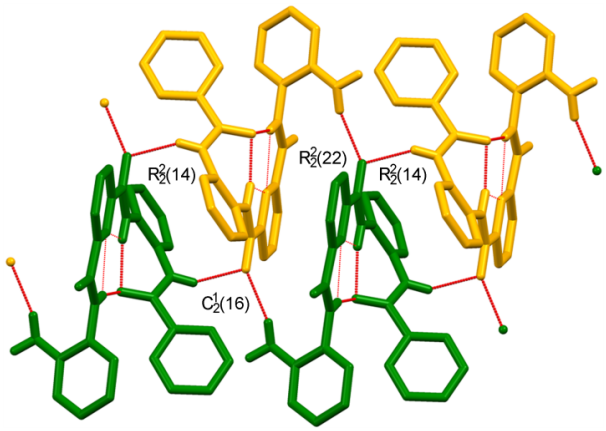

Fig. 3. Crystal packing of foldamer **3**. Two ring motifs form a double chain

based on the unit cell measurements, it was obtained from several solvents and diffusion crystallizations, whereas each of the other observed crystal forms, were only obtained once.

The crystal packing of foldamer **4** is defined by stacked pairs (Figure 4a), where the small CH_3-groups are efficiently nestled inside the dimer stabilized by two intermolecular hydrogen bonds ($R_2^2(32)$). The only example of an unpaired packing motif was seen with a DMSO solvate (**4**S_1-DMSO), where DMSO as a strong hydrogen bond acceptor forms a hydrogen bond to the foldamer (D motif) thus prohibiting the intermolecular hydrogen bonding network essential for the stacked pairs (Figure 4d).

Foldamer 5

Foldamers **5** and **6** also have electron donating aliphatic groups with increasing size and bulkiness at one end of the molecule. Foldamer **5** was the other foldamer of the series, which did not crystallize as solvates, but only as two polymorphic forms, one in an @´$_2$-conformation and the other in an S_1-conformation (Figure 4b and 4e). The steric hindrance of the larger alkyl group affects the details of both structures.

The @-conformer is stabilized by only two intramolecular hydrogen bonds and the alkyl end is slightly turned away from the fold interior. A double chain crystal packing motif ($C_2^2(23)$ motif, see ESI) contributes also to the stability of the @'$_2$-conformation. In the structure of **5**S_1-Form II stacked pairs are not possible because of the size of the isopropyl group. Instead, the foldamer molecules pack into parallel, displaced pairs ($R_2^2(14)$ motif). The structure contains small, non-solvent accessible voids (26 Å^3) and the packing coefficient is smaller in comparison with the polymorphic forms of foldamer **4** and that of **5**@´$_2$-Form I (Table 2), which suggests less efficient packing.

Foldamer 6

The crystallization experiments of foldamer **6** produced only one solvate and one unsolvated structure, both in the S_2-conformation, which is not observed with any other foldamer. The *tert*-butyl group causes considerable steric hindrance to the folding and is likely the main reason for the S_2-conformation (Table 1, Figure 4c and 4f). Exceptionally for the

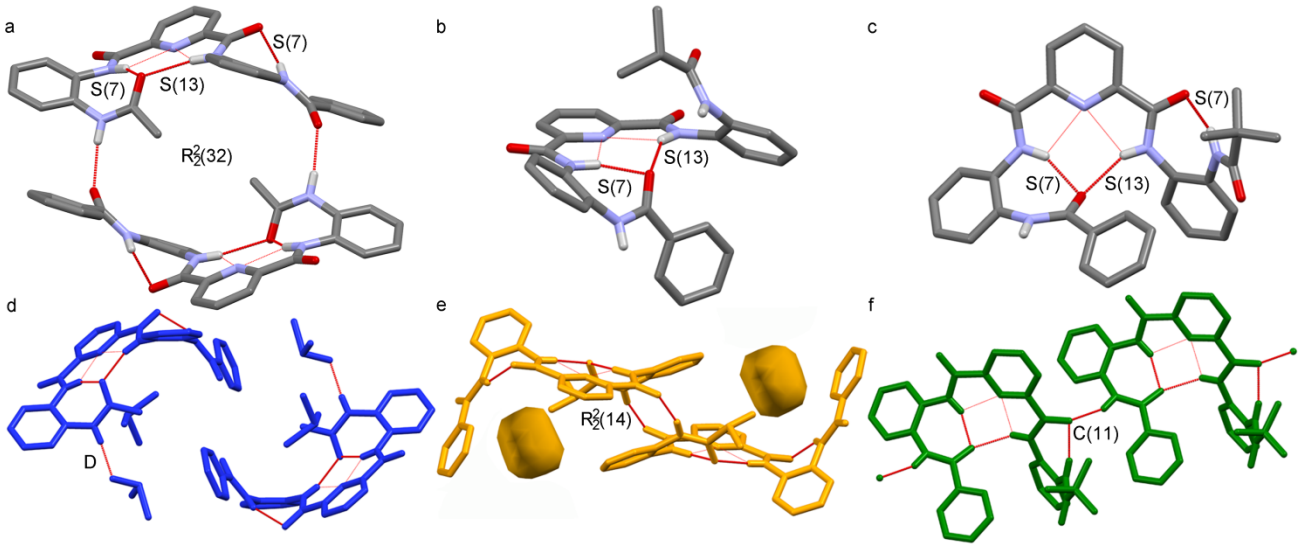

Fig. 4. a) Stacked pair ($R_2^2(32)$ motif) in **4S**$_1$-Form I, b) foldamer **5** in @'$_2$ conformation (**5@'**$_2$-Form I), c) foldamer **6** in the S_2 conformation (**6S**$_2$-Form I), d) unpaired DMSO solvate **4S**$_1$-DMSO (D motif), e) crystal packing of foldamer **5S**$_1$-Form II structure ($R_2^2(14)$ motif) showing non-solvent accessible voids, and f) chain-like crystal packing of foldamer **6** in **6S**$_2$-Form I (C(11) motif).

S-conformation, the foldamers pack into chains (C(11) motif). The reasons behind the unusual packing motif are not clear, but they could relate to the bulkiness of the *tert*-butyl group, as well as to the unique S_2-conformer.

Foldamer 7

Foldamer **7** has an electron density withdrawing cyano substituent at the other end of the molecule, which affects the electron density of the phenyl ring and the closest carbonyl group. Therefore, one could assume that @$_2$- and S_2-conformations were favoured, but the crystallization studies yielded only one unsolvated structure in the @$_2$-conformation and four solvates in the S_1-conformation, two of which are isomorphous (THF and DMA). Although the *p*-cyanophenyl ring is large and bulky, the planar shape and possibility for aromatic interactions stabilise the @-conformation and alleviate the steric hindrance. As typical, the @-conformation packs into chains and the S_1-conformers as parallel, displaced pairs with solvent accessible voids, where the solvent molecules are located in all structures. The S_1-conformation and parallel displaced pair motif are likely due to steric reasons caused by the size of the *p*-cyanophenyl group: stacked pairs could not form in S_1-conformation due to the size of the cyanophenyl groups.

Foldamer 8

Foldamer **8** is structurally very similar to foldamers **1** and **7**, but its solubility is much lower compared with the other foldamers and it only dissolved in DMSO, DMF and DMA. The methoxy group was designed to donate electron density to the carbonyl oxygen closest to it, but this small alteration in the structure caused that no crystal structures were obtained for foldamer **8**, which demonstrates how potent these small changes can be.

General trends in crystal packing and crystallization

General trends in the crystal packing show that the @-conformer enables slightly more efficient crystal packing, as the packing coefficients of the @-conformers are generally higher than the packing coefficients of the S-conformers (Table1, see ESI for average packing coefficients). This could relate to a looser and more open form of the S-conformer,

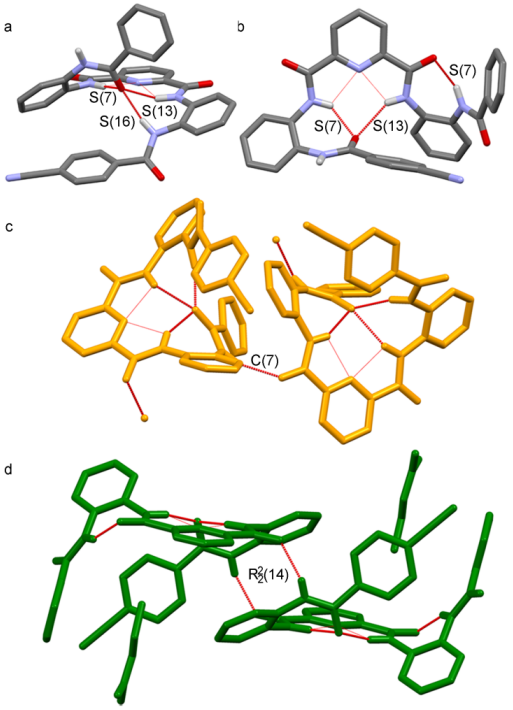

Fig. 5. Conformations and crystal packing of foldamer **7** a) **7@**$_2$-Form I, b) **7S**$_1$-EtOAc, c) chain structure of **7@**$_2$-Form I (C(7) motif) and d) pair structure of **7S**$_1$-EtOAc ($R_2^2(14)$ motif).

which together with the packing motif preferences may more easily lead to voids in the crystal structures.

The crystal packing of foldamers in the @-conformation favours the formation of continuous chains or discrete rings via hydrogen bonding (Figures 1-5, Table 1). Hydrogen bonding to chains likely gives more stability to the protocrystal and allows an easy addition of foldamer molecules to the crystal phase during the crystal formation. There are also several intermolecular π-stacking interactions in an average structure that contribute to the stability of the packing.

S-conformers tend to favour a pairwise crystal packing (Figures 2 and 4-5, Table 1). The S-conformation allows for efficient intermolecular pairing interactions thus creating a block-like unity that packs efficiently, but hinders the formation of hydrogen bonded chains like those in the @-conformation structures. Two types of paired structures were identified for the S-conformer structures; a stacked pair seen with the two smallest S-conformation foldamers **2** and **4** (Figure 2c and 4a) and a parallel displaced pair seen with foldamers **5** and **7** (Figure 4d and 5e). In a stacked pair the molecules are on top of each other whereas in a parallel displaced pair the molecules are only partially stacked. The parallel displaced pair allows enough space for larger substituents, but also leads to a void near the pair (Figure 4d and ESI). The size of the void depends on the substituents: in the case foldamer **7** with a large aromatic ring the void is solvent accessible, but in the case of the foldamer **5** with a smaller substituent the void is non-solvent accessible (26 $Å^3$).[24]

The effect of the solvent and other crystallization conditions on the preferred conformations or crystal forms is fairly difficult to evaluate. Foldamers **1** and **2** showed remarkable crystallization tendencies in various solvents producing a variety of structures, both unsolvated polymorphs and solvates, as well as many different crystal forms from same solvents. This indicates potential as co-crystal formers and small molecule or ion hosts. Foldamer **3**, on the other hand, had a surprisingly uniform crystallization behavior as it repeatedly produced only one crystal form regardless of the solvents used. The other four foldamers have produced almost equally unsolvated and solvated forms, but the crystal formation is not as easy as with foldamers **1** and **2**.

Conclusions

Altogether 33 different crystal structures for a series of seven oligoamide foldamers were crystallized and analyzed. The compounds were found to fold in two distinct conformations with some variance in their intramolecular hydrogen bonding patterns. The nuances of the conformations were affected not only by hydrogen bonding but also by steric hindrance and variance in the electronic environment caused by the substituents. These effects were the most evident for foldamer **8**, which did not crystallize at all. Nearly analogous foldamers **1** and **7**, both of which had much better solubility than foldamer **8**, produced readily good quality crystals from many different solvents. Although aromatic interactions were predicted to have effect on the conformation stability in previous DFT calculations,[20] their effect in crystal structures was not as obvious.

Two of the foldamers (**1** and **3**) fold exclusively to a protohelical @-conformation, and two (**4** and **6**) exclusively to an S-conformation. For the other three (**2**, **5** and **7**) both conformers were observed with no clear pattern on the conformational preferences. This indicates that the conformations are close in energy, as DFT calculations suggested, and that in solution both forms are likely present.

The tendency to form solvates varied. Foldamer **2** forms several solvates, mostly in the S-conformation; while the nearly identical foldamer **3** did not form any solvates and repeatedly produced the same crystal form despite the solvent used. Foldamer **1** has a strong tendency to form solvates, but exclusively in @-conformation.

The packing coefficients are slightly larger with @-conformer structures indicating denser packing without voids, whereas the voids in the S-conformer structures relate to pairwise packing leaving space for the solvent and inducing less dense packing. This trend is especially clear in the structures of foldamer **7**.

Oligoamide foldamers have proven to be a very fruitful source of crystallographic information, as they relatively easily produce good quality crystals in varying conditions and provide information on the subtle structural and environmental changes on the outcome of the solid state structures. Our future goal is to concentrate on the co-crystal and complex formation of the most versatile crystal formers, foldamers **1** and **2**, and, on the other hand, explore the uniform crystallization behavior of foldamer **3** and compare it with the conformational behavior in solution. This will clarify the reasons behind the crystal packing motifs and provide new insights for crystal engineering and crystal structure prediction.

Experimental

Materials and Methods

The oligoamide foldamers **1**,**2** and **4**-**8** (Scheme 1), as well as the intermediate products were prepared according to the literature procedures reported in our previous papers.[19,20] Compound **3** is previously unpublished and prepared according to the procedure outlined by Gunnlaugsson *et al.*[25] Details of the synthesis and characterization of foldamer 3 are presented in ESI.

X-Ray crystallography

The crystal data and data collection parameters are presented in Table 2 and crystallization solvents in Table 1. Analytical grade solvents and Millipore water were used for crystallizations. The details of all crystallization experiments are reported in ESI.

Single crystal X-ray diffraction data of structures **2**@-Form II, **2**@-DMA, **2**S-DCM-1, **2**S-DCM-2, **4**S_1-Form II, **4**S_1-diox **7**S_1-THF and **7**S_1-DMA were collected with a Bruker Nonius KappaCCD diffractometer using a Bruker AXS APEX II CCD detector.

Table 2. Crystal data and collection parameters 1.

	1@-Form II	**1@**-DMA*	**1@**-DMSO-H_2O	**2@**-form II	**2@**-DMA	**2S**-DCM-1
Formula	$3C_{33}H_{25}N_5O_4$	$C_{33}H_{25}N_5O_4$• C_4H_9NO	$C_{33}H_{25}N_5O_4$• C_2D_6OS•H_2O	$C_{26}H_{20}N_4O_3$	$C_{26}H_{20}N_4O_3$• C_4H_9NO	$C_{26}H_{20}N_4O_3$• CH_2Cl_2
Crystallization solvent	DMSO-d_6	DMA	DMSO-d_6	DMA	DMA	DCM
M/gmol^{-1}	555.58	642.70	657.76	436.46	523.58	521.39
Crystal system	Triclinic	Monoclinic	Monoclinic	Orthorhombic	Triclinic	Triclinic
Space group	P-1	$P2_1/c$	$P2_1/c$	Pbca	P-1	P-1
a/Å	13.0733(2)	14.34241(19)	14.5114(7)	10.9333(6)	8.1890(2)	8.9343(1)
b/Å	16.7932(3)	19.5568(2)	19.1956(7)	18.0540(11)	12.1939(3)	12.0833(1)
c/Å	19.0162(2)	11.34410(16)	11.3102(4)	21.5317(14)	14.5599(3)	13.1298(1)
α/º	91.0697(11)	90	90	90	68.849(2)	112.097(1)
β/º	94.1916(12)	94.0477(12)	97.975(4)	90	80.180(3)	93.024(1)
γ/º	103.0744(14)	90	90	90	86.555(3)	101.520(1)
V/Å^3	4053.08	3173.98(7)	3120.0(2)	4250.1(4)	1336.1(1)	1263.1(3)
Z	6	4	4	8	2	2
ρ_{calc}/g cm^{-3}	1.366	1.345	1.400	1.364	1.301	1.359
Meas. reflns	84317	35938	10673	6664	6464	5929
Indep. reflns	17003	7844	6291	3634	4349	4297
T/K	123	173	123	173	173	173
Radiation	CuKα	MoKα	CuKα	CuKα	CuKα	CuKα
λ/Å	1.5418	0.7107	1.5418	1.54178	1.54178	1.54178
Monochromation	Mirror	Mirror	Mirror	Graphite	Graphite	Graphite
Absorption correction	analytical	analytical	analytical	multi-scan	multi-scan	multi-scan
Abs. Corr. program	CrysalisPro[26]	CrysalisPro	CrysalisPro	Denzo-SMN 1997[27]	Denzo-SMN 1997	Denzo-SMN 1997
Refinement programs	SHELX-2013,[28] ShelXle[29]	SHELX-2013, ShelXle	SHELX-2013, ShelXle	SHELX-97[28]	SHELX-97	SHELX-97
R_{int}	0.0345	0.0224	0.0655	0.0578	0.0588	0.0863
R_1 [I> 2σ(I)]	0.0425	0.0424	0.0610	0.0543	0.0512	0.0657
wR_2 [I> 2σ(I)]	0.1137	0.0981	0.1416	0.1132	0.1195	0.1671
GooF	1.087	1.024	1.093	1.039	1.027	1.052
	2S-DCM-2	**3@**-Form I	**4S**$_1$-Form II	**4S**$_1$-Diox	**4S**$_1$-DMSO	**6S**$_2$-Diox
Formula	$C_{26}H_{20}N_4O_3$• $0.5CH_2Cl_2$	$C_{26}H_{21}N_5O_3$	$C_{28}H_{23}N_5O_4$	$C_{28}H_{23}N_5O_4$. $0.5C_4H_8O_2$	$C_{28}H_{23}N_5O_4$. $2C_2H_6SO$	$C_{31}H_{29}N_5O_4$• $0.5C_4H_8O_2$
Crystallization solvent	DCM	MeCN	EtOAc	1,4-dioxane	DMSO	1,4-dioxane
M/gmol^{-1}	478.92	451.48	493.51	537.57	649.77	579.64
Crystal system	Triclinic	Triclinic	Monoclinic	Triclinic	Triclinic	Triclinic
Space group	P-1	P-1	C2/c	P-1	P-1	P-1
a/Å	9.0133(1)	8.5193(3)	28.6348(11)	8.7193(2)	8.7246(5)	9.6881(6)
b/Å	11.9653(1)	9.8054(4)	8.6348(3)	13.1332(3)	13.2012(5)	10.6294(7)
c/Å	12.0000(1)	14.3709(4)	21.4506(10)	13.2791(5)	15.2754(5)	15.8346(9)
α/º	83.142(1)	74.437(3)	90	114.688(1)	97.888(3)	105.487(5)
β/º	81.233(1)	75.224(3)	94.284(2)	97.288(1)	105.934(4)	103.244(5)
γ/º	69.213(1)	78.208(3)	90	103.683(1)	104.062(4)	102.241(5)
V/Å3	1192.8(1)	1106.25(7)	4883.6(3)	1297.73(6)	1611.07(13)	1463.30(16)
Z	2	2	8	2	2	2
ρcalc/g cm^{-3}	1.333	1.355	1.342	1.376	1.339	1.316
Meas. reflns	5922	23956	6571	13017	11102	10347
Indep. reflns	4093	5460	4156	6647	7198	6610
T/K	173	173	173	173	173	173
Radiation	CuKα	MoKα	CuKα	MoKα	MoKα	MoKα
λ/Å	1.54178	0.7107	1.54178	0.71073	0.7107	0.7107
Monochromation	Graphite	Mirror	Graphite	Graphite	Mirror	Mirror
Absorption correction	multi-scan	multi-scan	multi-scan	multi-scan	multi-scan	multi-scan
Abs. Corr. program	Denzo-SMN 1997	CrysalisPro	Denzo-SMN 1997	Denzo-SMN 1997	CrysalisPro	CrysalisPro
Refinement programs	SHELX-97	SHELX-2013, ShelXle	SHELX-97	SHELX-97	SHELX-2013, ShelXle	SHELX-2013, ShelXle
Rint	0.0691	0.0265	0.0613	0.0700	0.0217	0.0222
R1 [I> 2σ(I)]	0.0582	0.0439	0.0518	0.0586	0.0516	0.0580
wR2 [I> 2σ(I)]	0.1498	0.1054	0.1129	0.1308	0.1138	0.0991
GooF	1.049	1.100	1.072	1.062	1.031	1.037

* Crystal data of the isomorphous solvate structures (acetone and acetonitrile solvates) are presented in the ESI.

Table 2. continued

	7S$_1$-$CHCl_3$	**7S**$_1$-DMA*
Formula	$C_{35}H_{25}N_6O_4$•$CHCl_3$	$C_{35}H_{25}N_6O_4$•C_4H_9ON
Crystallization solvent	$CHCl_3$	DMA
M/gmol^{-1}	699.96	667.71
Crystal system	Monoclinic	Monoclinic
Space group	$P2_1/n$	$P2_1/n$
a/Å	12.3983(2)	12.1856(5)
b/Å	19.7518(3)	20.3897(8)
c/Å	14.0691(2)	13.7195(5)
α/º	90	90
β/º	99.8562(16)	95.426(3)
γ/º	90	90
V/Å^3	3394.52(10)	3393.5(2)
Z	4	4
ρ_{calc}/g cm^{-3}	1.370	1.307
Meas. reflns	13725	9461
Indep. reflns	7694	5424
T/K	173	173
Radiation	MoKα	CuKα
λ/Å	0.7107	1.54178
Monochromation	Mirror	Graphite
Absorption correction	multi-scan	multi-scan
Abs. Corr. program	CrysalisPro	Denzo-SMN 1997
Refinement programs	SHELX-2013, ShelXle	SHELX-97
R_{int}	0.0161	0.0877
R_1 [I> 2σ(I)]	0.0501	0.0703
wR_2 [I> 2σ(I)]	0.1198	0.1653
GooF	1.024	1.021

* Crystal data of the isomorphous THF solvate is presented in the ESI.

The crystal structures of **1**@-MeCN, **1**@-Form II, **1**@-Ac and **1**@-DMSO-H_2O were measured with an Agilent Supernova Dualsource diffractometer using an Agilent Atlas CCD detector. The crystal structures of **1**@-DMA, **3**@-Form I, **4**S$_1$-DMSO, **6**S$_2$-Diox and **7**S$_1$-$CHCl_3$ were measured with an Agilent Supernova diffractometer using an Agilent Eos CCD detector. The structures were solved with direct methods and refined using Fourier techniques. All non-hydrogen atoms were refined anisotropically and the hydrogen atoms were placed in idealized positions except for N-H and H_2O hydrogen atoms which were found from the electron density map, and included in the structure factor calculations. Details of the crystal data and the refinement are presented in Table 2 and ESI.

The crystal structures were analysed by calculating the packing coefficients.[30] Graph set symbols[31,32] for hydrogen bonding were assigned and used to compare the hydrogen bonding between the different crystal structures.

Structures **2**@-Form I, **2**S-MeCN, **2**@-S-DMF, **4**S$_1$-Form I, **5**@'$_2$-Form I, **5**S$_1$-Form II, **6**S$_2$-Form I, **7**@$_2$-Form I and **7**S$_1$-EtOAc included in the discussion were published in our previous paper[20] and their details can be found there or free of charge from the Cambridge Crystallographic Data Centre via www.ccdc.cam.ac.uk/data request/cif, CCDC-1038215-1038223.

Notes and references

1 S. H. Gellman, *Acc. Chem. Res.*, 1998, **31**, 173.

2 D. J. Hill, M. J. Mio, R. B. Prince, T. S. Hughes and J. S. Moore, *Chem. Rev.*, 2001, **101**, 3893.

3 P. Claudon, A. Violette, K. Lamour, M. Decossas, S. Fournel, B. Heurtault, J. Godet, Y. Mély, B. Jamart-Grégoire, M.-C. Averlant-Petit, J.-P. Briand, G. Duportail, H. Monteil and G. Guichard, *Angew. Chem., Int. Ed.*, 2010, **49**, 333.

4 R. R. Araghi and B. Koksch, *Chem. Comm*, 2011, **47**, 3544.

5 J. Zhu, R. D. Barra, H. Zeng, E. Skrzypczak-Jankun, X. C. Zeng and B. Gong, *J. Am. Chem. Soc.*, 2000, **122**, 4219.

6 A. J. Neuvonen and P. M. Pihko, *Org. Lett.*, 2014, **16**, 5152.

7 N. Probst, Á. Madarász, A. Valkonen, I. Pápai, K. Rissanen, A. Neuvonen and P. M. Pihko, *Angew, Chem. Int. Ed.*, 2012, **51**, 8495.

8 V. Berl, I. Huc, R. G. Khoury and J.-M. Lehn, *Chem. Eur. J.*, 2001, **7**, 2798.

9 V. Berl, I. Huc, R. G. Khoury and J.-M. Lehn, *Chem. Eur. J.*, 2001, **7**, 2810.

10 I. Huc, V. Maurizot, H. Gornitzka and J.-M. Léger, *Chem. Commun.*, 2002, **6**, 578.

11 B. Baptiste, J. Zhu, D. Haldar, B. Kauffmann, J.-M. Léger and I. Huc, *Chem. Asian J.*, 2010, **5**, 1364.

12 H. Jiang, J.-M. Léger and I. Huc, *J. Am. Chem. Soc.*, 2003, **125**, 3448.

13 E.R. Gillies, C. Dolain, J.-M. Léger and I. Huc, *J. Org. Chem.*, 2006, **71**, 7931.

14 N. Delsuc, J.-M. Léger, S. Massip and I. Huc, *Angew. Chem. Int. Ed.*, 2007, **46**, 214.

15 D. Sánchez-Garcia, B. Kauffmann, T. Kawananni, H. Ihara, M. Takafuji, M.-H. Delville and I. Huc, *J. Am. Chem. Soc.*, 2009, **131**, 8642.

16 Y. Ferrand, A. M. Kendhale, J. Garric, B. Kauffman and I. Huc, *Angew. Chem. Int. Ed.*, 2010, **49**, 1778.

17 Y. Hamuro, S. J. Geib and A. D. Hamilton, *J. Am. Chem. Soc.*, 1996, **118**, 7529.

18 Y. Hamuro, S. J. Geib and A. D. Hamilton, *J. Am. Chem. Soc.*, 1997, **119**, 10587.

19 A. Suhonen, E. Nauha, K. Salorinne, K. Helttunen and M. Nissinen, *CrystEngComm*, 2012, **14**, 7398.

20 M. Kortelainen, A. Suhonen, A. Hamza, I. Pápai, E. Nauha, S. Yliniemelä-Sipari, M. Nissinen and P. Pihko, Chem. Eur. J., 2015, **21**, 9493.

21 P. M. Pihko, S. Rapakko and R. K. Wierenga, in *Hydrogen Bonding in Organic Synthesis*, ed. P.M. Pihko, WILEY-VCH Verlag GmbH & Co. KGaA, Weinheim, Germany, 2009, pp. 43.

22 K. Mitsui, S.A. Hyatt, D.A. Turner, C.M. Hadad, J.R. Parquette, *Chem. Commun.* **2009**, 3261.

23 N.T. Salzameda, D.A. Lightner, *Monatsh. Chem.* **2007**, *138*, 237

24 A. L. Spek, *Acta Cryst. D*, 2009, **65**, 148.

25 F. Stomeo, C. Lincheneau, J. P. Leonard, J. E. O'Brien, R. D. Peacock, C. P. McCoy and T. Gunnlaugsson, *J. Am. Chem. Soc.*, 2009, **131**, 9636.

26 Agilent (2011), CrysAlisPRO, Agilent Technologies UK Ltd, Yarnton, England.

27 Z. Otwinowski, D. Borek, W. Majewski and W. Minor, *Acta Crystallogr. A.*, 2003, **59**, 228.

28 G. M. Sheldrick, *Acta Crystallogr. A.*, 2008, **64**, 112.

29 C. B. Hübschle, G. M. Sheldrick and B. Dittrich, *J. Appl. Cryst.*, 2011, **44**, 1281.
30 A. I. Kitaĭgorodskiĭ, Organic Chemical Crystallography, Consultants Bureau, New York, 1961.
31 M. C. Etter and J. C. MacDonald, *Acta Crystallogr., Sect. B: Struct. Sci.*, 1990, **46**, 256.
32 J. Bernstein, R. E. Davis, L. Shimoni and N.-L. Chung, *Angew. Chem., Int. Ed.*, 1995, **34**, 1555.